Antisense lncRNAs expression correlates with attenuation of highly transcribed genes in fission yeast

Maxime Wery[1], Camille Gautier[1], Marc Descrimes[1], Mayuko Yoda[1], Valérie Migeot[2], Damien Hermand[2] and Antonin Morillon[1,3]

[1] ncRNA, epigenetic and genome fluidity, Institut Curie, PSL Research University, CNRS UMR 3244, Université Pierre et Marie Curie, 26 rue d'Ulm, 75248 Paris Cedex 05, France

[2] URPHYM, Namur Research College (NARC), University of Namur, Namur 5000, Belgium

[3] Corresponding author

Running title: Transcription regulation by aslncRNA in *S. pombe*

Keywords: antisense lncRNA/*ctt1*/Exo2/NET-Seq/XUT/*S. pombe*

ABSTRACT

Antisense (as) lncRNAs can regulate gene expression but whether this occurs at the transcriptional or post-transcriptional level remains unclear. Furthermore, the molecular bases for aslncRNAs-mediated regulation remain incomplete. Here, we report that inactivation of the cytoplasmic exoribonuclease Exo2 results confers sensitivity to oxidative stress in fission yeast. Mechanistic investigations revealed that induction of the catalase-coding gene *ctt1* is impaired in *exo2Δ* cells, correlating with the accumulation an Exo2-sensitivite lncRNA (XUT), antisense to *ctt1*. Interestingly, expression of the asXUT was also activated in wild-type cells upon oxydative stress, concomitant to *ctt1* induction, indicating a potential attenuation feedback. This attenuation is Dicer-independent, characterized by low RNAPII-ser5 phosphorylation and requires histone deacetylase activity. Using Native Elongating Transcript sequencing in *exo2Δ* cells, we revealed asXUT-associated attenuation for a subset of highly transcribed genes displaying prominent promoter-proximal nucleosome depletion and histone acetylation, suggesting that asXUTs attenuate genes whose transcription exceeds a critical threshold. We propose that asXUT could mediate transcriptional regulation *via* sense-paired gene promoter features using a general conserved mechanism, independent of RNAi.

INTRODUCTION

Eukaryotic genomes are pervasively transcribed (Clark et al, 2011), generating plenty of non-coding (nc) transcripts, distinct from the housekeeping rRNAs, tRNAs and sn(o)RNAs, and that are arbitrarily classified into small (< 200 nt) and long (≥ 200 nt) ncRNAs (Jarroux et al, 2017; Wery et al, 2011).

Long (l)ncRNAs are produced by RNA polymerase II (RNAPII), capped and polyadenylated, yet lack protein-coding potential (Guttman et al, 2009; Khalil et al, 2009), although this last point is subject to exceptions (de Andres-Pablo et al, 2017).

Several lines of evidence suggest that they are functionally important. First, lncRNAs show tissue-specific expression (Djebali et al, 2012) and respond to diverse stimuli, such as oxidative stress (Giannakakis et al, 2015), suggesting that their expression is precisely controlled. Second, several lncRNAs are misregulated in diseases including cancer and neurological disorders (Renganathan & Felley-Bosco, 2017; Saha et al, 2017; Schmitt & Chang, 2016). Furthermore, there is a growing repertoire of cellular processes in which lncRNAs play important roles, including X-chromosome inactivation, imprinting, maintenance of pluripotency and transcriptional regulation (Mercer et al, 2009; Rinn & Chang, 2012).

Several classes of lncRNAs have been described (Jarroux et al, 2017). Among them, large intervening non-coding (linc)RNAs, which result from transcription of intergenic regions, have attracted a lot of attention as being involved in *cis*- and *trans*-regulation, mostly at the chromatin level, of genes important for development and cancer (Rinn & Chang, 2012).

Another class of lncRNAs consists in antisense transcripts, that are produced from DNA strand antisense to genes (Pelechano & Steinmetz, 2013). Several examples of regulatory antisense (as)lncRNAs acting on sense gene expression in *cis* or in *trans* have been described in the budding yeast *Saccharomyces cerevisiae* (Berretta et al, 2008; Camblong et al, 2009; Camblong et al, 2007; Houseley et al, 2008; Pinskaya et al, 2009; Uhler et al, 2007; van Werven et al, 2012), in the fission

yeast *Schizosaccharomyces pombe* (Bitton et al, 2011; Leong et al, 2014), in plant (Swiezewski et al, 2009) and in mammalian cells (Lee & Lu, 1999; Yap et al, 2010).

Our previous studies in budding and fission yeasts revealed that aslncRNAs are globally unstable and are mainly targeted by the cytoplasmic 5'-3' RNA decay pathway dependent on the Xrn1 and Exo2 exoribonucleases in *S. cerevisiae* (Van Dijk et al, 2011; Wery et al, 2016) and *S. pombe* (Wery et al, 2017), respectively. Inactivation of Xrn1/Exo2 leads to the stabilization of a family of lncRNAs, referred to as Xrn1-sensititve Unstable Transcripts (XUTs), the majority of which are antisense to protein-coding genes (Van Dijk et al, 2011; Wery et al, 2016; Wery et al, 2017). Interestingly, in *S. cerevisiae*, we defined among these antisense (as)XUTs a subgroup for which the sense-paired genes (referred to as class 1) undergo antisense-mediated transcriptional silencing (Van Dijk et al, 2011). However, the molecular mechanism by which asXUTs could regulate sense gene expression remains largely unknown to date, still interrogating whether sense transcription is impaired at the initiation and/or elongation and/or termination stages, whether any post-transcriptional event is in play, and whether the epigenetic landscape contributes in the regulatory determinants. In addition, such a transcriptional aslncRNA-mediated regulation has not been documented yet in *S. pombe*, where RNAi could potentially contribute to the regulation.

Here we show that the catalase-coding gene *ctt1* in fission yeast is transcriptionally attenuated upon oxidative stress when its paired-asXUT is stabilized. Mechanistic characterization revealed that this process is RNAi-independent, characterized by low RNAPII Ser5-phosphorylation (Ser5-P) and mediated by histone deacetylase (HDAC) activity. Using Native Elongating Transcript sequencing, we identified class 1 as a subset of highly transcribed genes, with particular epigenetic marks, showing transcriptional attenuation upon stabilization of their paired-asXUTs. Our data support a model where asXUTs could modulate expression of their associated sense genes, only when expression exceeds a critical threshold, using a conserved mechanism independent of RNAi.

RESULTS

Exo2-deficient cells are sensitive to hydrogen peroxide and defective for *ctt1* induction upon oxidative stress

In a preliminary phenotypical characterization, we observed that in addition to the previously described temperature sensitivity (Szankasi & Smith, 1996), *exo2Δ* cells were sensitive to H_2O_2 (Figure 1A).

Survival to oxidative stress upon exposure to H_2O_2 requires an enzyme known as catalase (Mutoh et al, 1999), which is encoded by the *ctt1* gene in fission yeast and is strongly induced in response to H_2O_2 treatment (Nakagawa et al, 1995). We analyzed *ctt1* mRNA induction in WT and *exo2Δ* cells. Northern-blot (Figure 1B) and RT-qPCR kinetics analyses (Supplementary Figure S1A-B) showed that *exo2Δ* exhibits a 3-fold reduction in induction rate, with a peak of induction reached 15 minutes after H_2O_2 addition *vs* 10 for the WT (Supplementary Figure S1A).

Thus, full induction of *ctt1* upon addition of H_2O_2 requires Exo2.

Antisense XUT attenuates *ctt1* upon stress-mediated induction independently of RNAi

In fission yeast, loss of Exo2 leads to the stabilization of 1638 Xrn1/Exo2-sensitive Unstable Transcripts (XUTs), most of which are antisense to protein-coding gene (Wery et al, 2017). Analysis of the annotation revealed that *ctt1* has an antisense (as)XUT, namely *XUT0794* (Figure 1C).

We hypothesized that *XUT0794* could directly control *ctt1* expression or provide substrate for siRNA-mediated silencing. To discriminate between these possibilities, we tested whether *ctt1* attenuation requires Dicer. As shown in Figure 1D, *ctt1* attenuation was not suppressed in the *exo2Δ dcr1Δ* double mutant. Conversely, Dicer overexpression in *exo2Δ* cells had no impact on *ctt1* attenuation (Supplementary Figure S1C-E). These data indicate that Dicer is not necessary to the regulation, which is consistent with the observation that asXUTs are globally not targeted by RNAi in *S. pombe* (Wery et al, 2017).

Strikingly, *XUT0794* was also activated upon oxidative stress in a WT context (Figure 1E). Furthermore, its peak of induction was reached very rapidly (5 min), before the *ctt1* mRNA peak (10 min), suggesting that it might be part of a natural attenuation mechanism (feedback loop) for *ctt1* expression.

In summary, our data suggest that *ctt1* induction requires Exo2 activity for maintaining a low level of a XUT antisense to *ctt1*. Upon induction, the XUT is activated and could modulate expression of *ctt1*, in a similar way as shown for asXUT-associated genes in *S. cerevisiae*, such as *GAL1-10* (Houseley et al, 2008; Pinskaya et al, 2009).

Efficiency of *ctt1* attenuation correlates with antisense *XUT0794* abundance

In order to test whether *ctt1* attenuation directly depends on antisense *XUT0794* and is not an indirect effect of *exo2Δ*, we overexpressed the XUT in *cis*, in WT cells, using a regulatable *P41nmt1* promoter (Supplementary Figure 2A). Upon promoter activation, *XUT0794* accumulated and *ctt1* was not induced in response to H_2O_2 (Supplementary Figure 2A). However, in this context, *ctt1* silencing might result from transcriptional interference. Note that expression of the XUT in *trans* had no effect on *ctt1* induction (Supplementary Figure 2B).

We also tried to disrupt *XUT0794* promoter using a *kan*^{R} marker. Unexpectedly, this failed to repress *XUT0794*. Instead, *ctt1-kan*^{R} cells accumulated *XUT0794* in absence of H_2O_2 more than *exo2Δ* cells, and *ctt1* mRNA was attenuated upon oxidative stress (Supplementary Figure 2C).

As a third strategy, we inserted a self-cleaving hammerhead ribozyme (RZ) at position 254/815 of *XUT0794* (Figure 2A) and integrated the construct at the *ctt1* locus in WT and *exo2Δ* strains, without any manipulation of *XUT0794* promoter. In the WT + RZ context, neither the 5' nor the 3' fragment of *XUT0794* accumulated (Figure 2B), and *ctt1* induction was similar to WT cells (Figure 2C). In the *exo2Δ* + RZ context, the 5' fragment was not detected, but the 3' fragment accumulated 5x more than in *exo2Δ* without RZ (Figure 2B). This imbalance between the two RNA parts indicates that RZ was efficiently cleaved, the 5' fragment being presumably degraded (Khvorova

et al, 2003) while the 3' fragment accumulated. Importantly, the higher abundance of the 255-815 fragment of *XUT0794* in *exo2Δ* + RZ cells compared to *exo2Δ* without RZ correlated with a significantly stronger attenuation of *ctt1* (Figure 2C).

We conclude that the 255-815 fragment of *XUT0794* is sufficient to attenuate *ctt1* and that the efficiency of attenuation depends on the abundance of the antisense XUT, which is consistent with our hypothesis that the regulation is mediated by the RNA itself and is not an indirect effect of Exo2 inactivation.

XUT-mediated transcriptional attenuation of *ctt1* is characterized by partial RNAPII Ser5 phosphorylation

To determine whether *ctt1* attenuation occurs at the transcriptional level, we performed RNAPII ChIP experiments in WT and *exo2Δ* cells. In oxidative stress conditions, RNAPII occupancy in the mutant showed a significant 2- to 4-fold decrease along the *ctt1* locus (Figure 3A-B), indicating that the attenuation is transcriptional.

Analysis of the distribution of differentially phosphorylated forms of RNAPII largest subunit CTD provided further insights into the mechanism of transcriptional attenuation. Ser5-P is associated to initiation of transcription and predominates in the promoter-proximal region of the gene, while Ser2-P is associated to transcription elongation and increases along the gene core (Drogat & Hermand, 2012). Upon oxidative stress, we observed a 30% decrease of Ser5-P RNAPII in the 5' and core regions of *ctt1*, in the *exo2Δ* mutant (Figure 3C). In contrast, Ser2-P RNAPII occupancy was similar in the two strains (Figure 3D).

In summary, stabilization of *XUT0794* impairs the early stage of *ctt1* transcription, with less RNAPII loaded on the gene in response to oxidative stress and an additional reduced level of Ser5-P.

XUT-mediated attenuation of *ctt1* depends on histone deacetylation

Several studies in budding yeast have pointed out the role of HDAC, including the class II HDAC Hda1, in antisense lncRNA-mediated gene silencing (Berretta et al, 2008; Camblong et al, 2007; Houseley et al, 2008). To test whether asXUT-mediated attenuation of *ctt1* depends on HDAC activity, WT and *exo2Δ* cells were treated with trichostatin A (TSA), an inhibitor of class I-II HDAC. When exposed to oxidative stress, TSA-treated *exo2Δ* cells accumulated *ctt1* mRNA to the same level as the control (DMSO-treated) WT strain (Figure 4A). We also noted that the uninduced level of *ctt1* mRNA was increased in the TSA-treated WT and *exo2Δ* cells, indicating that *ctt1* repression requires an HDAC activity. Furthermore, both *ctt1* mRNA and *XUT0794* levels in TSA-treated WT cells showed a 2-fold increase compared to the DMSO-treated control after H_2O_2 addition (Figure 4A-B). This indicates that the *XUT0794*-depending feedback loop that should modulate *ctt1* expression in WT cells upon exposure to H_2O_2 is impaired when HDAC activity is inhibited.

Based on this observation, we predicted histone acetylation along *ctt1* to be affected upon *XUT0794* stabilization. ChIP experiments in *ctt1* induction conditions revealed a significant 50% and 30% reduction of histone H4K5/8/12/16 acetylation and H3K14 acetylation, respectively, in the *exo2Δ* mutant, in the region where *ctt1* gene and *XUT0794* overlap (Figure 4C-D, probe C). These data support the idea that XUT-mediated gene attenuation depends on HDAC, resulting in reduced levels of histone acetylation.

In an attempt to identify the HDAC involved, we tested the effect of Clr3 (the ortholog of Hda1), the class I HDAC Hos2 and the ING family protein Png2, a non-essential subunit of the Clr6 complex I (Nicolas et al, 2007). Attenuation of *ctt1* was not suppressed in the *exo2Δ clr3Δ*, *exo2Δ hos2Δ* and *exo2Δ png2Δ* mutants (Supplementary Figure 4A-C), indicating that none of the three tested factors is involved in the attenuation mechanism. The *png2Δ* single mutant exhibited a strong defect of *ctt1* induction and was synergic with *exo2Δ* (Supplementary Figure 4C), suggesting that both Exo2 and Png2 are required for efficient *ctt1* induction but act independently.

In conclusion, XUT-mediated attenuation of *ctt1* requires a HDAC activity, suggesting that mechanisms of regulation of gene expression by lncRNAs have been conserved across the yeast

clade, cryptic antisense lncRNAs attenuating expression of their paired-sense gene in a HDAC-dependent manner.

Antisense XUT-associated transcriptional gene attenuation in fission yeast

The data above show that *ctt1* is attenuated when its paired-asXUT is stabilized in *exo2Δ* cells, and the attenuation occurs at the level of transcription. We ask whether other genes are transcriptionally attenuated upon stabilization of their paired-asXUT. In *S. cerevisiae*, such genes have been previously identified using RNAPII ChIP-Seq, constituting the so-called 'class 1' (Van Dijk et al, 2011).

To identify class 1 genes in *S. pombe*, here we performed NET-Seq analysis in WT and *exo2Δ* cells. Although global mRNA synthesis was found to be unchanged upon *exo2* inactivation (Supplementary Figure S5A), differential expression analysis discriminated genes for which transcription in *exo2Δ* was significantly reduced (classes 1 & 2, n=723) or not (classes 3 & 4, n=4405). Within each category, we distinguished genes with (classes 1 & 3) or without (classes 2 & 4) asXUTs (Figure 5A-B; lists in Tables S1-4).

175 of the 723 genes transcriptionally attenuated in *exo2Δ* have asXUTs (class 1). Despite the proportion of class 1 genes among the attenuated genes is limited (24.2%), it is significantly higher than expected if presence of asXUT and sense gene attenuation were independent (Chi-square test, $P = 0.03$), suggesting that the attenuation depends on the stabilized asXUTs, at least in some cases. On the other hand, the transcriptional down-regulation of class 2 (no asXUT) is likely to be an indirect effect reflecting the slow growth phenotype of the *exo2Δ* mutant (Szankasi & Smith, 1996). This hypothesis is supported by the observation that class 2 is significantly enriched for GO terms "ribosome biogenesis" ($P=1.36e^{-08}$) and "cellular component biogenesis ($P= 1.04e^{-02}$), the expression levels of genes involved such biological processes directly depending on the growth rate (Kief & Warner, 1981). Altogether, these observations suggest that for a subgroup of genes, stabilization of the asXUT might contribute to attenuate transcription of the paired-sense gene.

Both classes 1 and 3 have asXUTs, but only class 1 is transcriptionally attenuated upon asXUTs stabilization. This suggests the existence of specificities discriminating the two classes. Indeed, in WT cells, class 1 is transcribed to higher levels than class 3 (Figure 5C), the latter actually showing the lowest transcription levels among the four classes (Supplementary Figure S5B). In *exo2Δ*, transcription of class 1 falls to the low, basal level of class 3 (Figure 5D). Notably, transcription of XUTs antisense to class 1 and 3 genes is similar in the WT and *exo2Δ* conditions (Supplementary Figure S5C), indicating that XUTs accumulation in *exo2Δ* is due to the inactivation of their decay and not to a global increase of their synthesis (Figure 5E).

Remarkably, in WT cells, the nascent antisense transcription signal surrounding the TSS of class 1 genes is higher than for class 3 (Figure 5F; see also Supplementary Figure 5D). This suggests that sense TSS overlap also constitutes a key factor for the potential regulatory activity of the XUTs antisense to class 1 genes.

At the chromatin level, class 1 shows a more pronounced nucleosome depletion in the TSS-proximal region than class 3 (Figure 6A), higher H3K14 (Figure 6B) and H4K5/8/12/16 acetylation (Figure 6C). Notably, when compared to the four classes, levels of histone acetylation at the TSS-proximal region were similar in classes 1 and 2 (Figure 6B-C).

Together, these results show that transcriptional attenuation could be associated with asXUT stabilization in fission yeast, suggesting that asXUT-mediated gene regulation is functionally conserved. We defined class 1 as highly transcribed genes, characterized by high promoter-proximal antisense nascent transcription and high histone acetylation levels. Upon asXUT stabilization, class 1 transcription decreases to basal levels, suggesting that asXUTs might be involved in the modulation of sense genes expression.

DISCUSSION

In this report, we show that induction of the catalase-coding gene *ctt1* in response to oxidative stress is impaired in cells inactivated for the Exo2-dependent 5'-3' cytoplasmic RNA decay pathway. This attenuation of *ctt1* correlates with the accumulation of an unstable Exo2-sensitive aslncRNA (*XUT0794*). Interestingly, antisense *XUT0794* also rapidly accumulated in WT cells after H_2O_2 addition, suggesting that it could participate in the modulation of *ctt1* induction. In this respect, a recent study in human fibroblasts has identifed a class of stress-induced aslncRNAs, which are activated upon oxidative stress (Giannakakis et al, 2015), suggesting that aslncRNAs induction might be part of a conserved response to oxidative stress in Eukaryotes.

Our data indicate that asXUT-associated regulation of *ctt1* (*i*) is independent of RNAi, which is consistent with the observations that asXUTs are not targeted by Dicer in fission yeast (Wery et al, 2017), (*ii*) occurs at the early transcriptional level, (*iii*) and is mediated by HDAC activity. Our attempts to identify the HDAC involved were unsuccessful, probably due to redundancy of HDAC activities. On the other hand, we could not test the role of the Set2 histone-methyltransferases due to lethality of the *exo2Δ set2Δ* mutant in our hands. Further mutational strategies would be required to address this question, as alternative models propose that it is antisense transcription itself, rather than the antisense lncRNA, that promotes histone deacetylation *via* Set2-mediated H3K36 methylation, which is coupled to RNAPII transcription and recruits HDAC complexes (Venkatesh & Workman, 2013). However, the observation at the genome-wide level that class 1 genes are attenuated upon accumulation of the associated antisense lncRNAs, while antisense transcription is unchanged, suggests that in this case, this is the RNA itself, rather than antisense transcription, that is important for the HDAC-mediated gene attenuation. Future mechanistic studies will be required to confirm this hypothesis. This will necessitate the implementation in fission yeast of techniques developed in *S. cerevisiae* to strand-specifically block aslncRNA synthesis (Huber et al, 2016; Lenstra et al, 2015), which remains technically challenging to date. For instance, a recent report revealed that

at some loci, the CRISPR interference approach is not strand-specific and results in the production of novel isoforms of the targeted aslncRNA (Howe et al, 2017).

Using NET-Seq in *exo2Δ* cells, we defined class 1 in *S. pombe*, *ie* those genes showing transcriptional attenuation upon stabilization of their paired-asXUT. Importantly, asXUT presence and sense gene attenuation in *exo2Δ* are not independent, supporting the idea that the regulation is mediated by the stabilized asXUTs and is not a side effect of Exo2 inactivation. Additional mechanistic analyses are required to confirm this hypothesis.

In our recent report, we showed show that genes with asXUT are globally less transcribed that genes without asXUT and that histone acetylation was reduced at their promoter but increased along the gene body (Wery et al, 2017). Here we show that genes with asXUT can be separated into two distinct classes, namely class 1 and class 3, according to their transcriptional attenuation or not upon stabilization of their paired-asXUT, respectively. Class 1 is highly transcribed and shows strong nucleosome depletion and high levels of histone acetylation at the promoter. In addition, class 1 displays high TSS-proximal antisense transcription, pointing the TSS region as a possible determinant for aslncRNA-mediated regulation. In contrast, class 3 is weakly transcribed, with poor promoter-proximal nucleosome depletion and low histone acetylation. Upon stabilization of asXUTs, transcription of class 1 drops down to the basal levels of class 3. This suggests the existence of a regulatory threshold, *ie* asXUTs would modulate expression of their associated sense genes, only if expression is above this threshold (Figure 7). This contrasts with a previous model based on the analysis of sense-antisense RNA levels in budding yeast, which proposed that antisense-mediated repression would be restricted to low sense expression, with no effect on highly expressed genes (Xu et al, 2011).

Our model suggests that at least a subset of asXUTs could regulate gene expression at the transcriptional level, reducing sense transcription, as shown previously in *S. cerevisiae* (Berretta et al, 2008; Van Dijk et al, 2011). In addition, XUTs could also act at other steps of the gene expression process, especially at the post-transcriptional level. In this regard, aslncRNAs have been shown to

modulate protein production in response to osmotic stress in *S. pombe* (Leong et al, 2014). In *S. cerevisiae*, a recent study showed that disruption of several aslncRNAs results into increased protein synthesis from their paired-sense mRNAs, indicating a role of these aslncRNAs in the control of protein abundance (Huber et al, 2016). Future investigations will be required to demonstrate the regulatory potential of asXUTs and to determine the step(s) of the gene expression process they act on.

In conclusion, our works in budding and fission yeasts show that the cytoplasmic 5'-end RNA decay plays a key role in controlling aslncRNAs endowed with a regulatory potential. Given the high conservation of Xrn1 in Eukaryotes, it is tempting to speculate that asXUTs and their regulatory activity are conserved in higher eukaryotes, contributing in buffering genome expression, and adding another layer to the complexity of gene regulation.

MATERIALS & METHODS

Yeast strains, plasmids and media

All the strains used in this study are listed in Supplementary Table S5. Mutant strains were constructed by meiotic cross or transformation, and verified by PCR on genomic DNA. Plasmid pAM353 for expression of *XUT0794* in *trans* was constructed by cloning *XUT0794* in the SalI site of pREP41 (*ars1 LEU2 P41nmt1*). Sanger sequencing confirmed the correct orientation of the insert and the absence of mutation. Hammerhead ribozyme (Libri et al, 2002) was inserted in *XUT0794* by two-step PCR, giving a 3.2 Kb final product corresponding to *ctt1* mRNA coordinates +/- 500 bp that was cloned in pREP41. After verification of absence of additional mutations by Sanger sequencing, the ribozyme-containing construct was excised and transformed in the YAM2534 strain (*ctt1::ura4*). Transformants were selected on 5-FOA plates and analyzed by PCR on genomic DNA. Deletion of *exo2* was performed subsequently.

Strains were grown at 32°C to mid-log phase (OD_{595} 0,5) in YES or EMM-L medium. For *ctt1* induction, 1 mM H_2O_2 was added for 15 minutes (Calvo et al, 2012), or different time points for analysis of kinetics of induction. Expression from *P41nmt1* was repressed by growing cells in EMM-L + 15 µM thiamine for 24 hours.

NET-Seq

NET-Seq libraries were constructed from biological duplicates of YAM2507 (*exo2Δ rpb3-flag*) cells and sequenced as previously described (Wery et al, 2017). Libraries for the WT strain YAM2492 (*rpb3-flag*) were described in the same previous report (Wery et al, 2017).

After removal of the 5'-adapter sequence, reads were uniquely mapped to the reference genome (ASM294v2.30) using version 0.12.8 of Bowtie (Langmead et al, 2009), with a tolerance of 2 mismatches.

Differential analysis was performed between the IP samples from WT and *exo2Δ* using DESeq (Anders & Huber, 2010). Genes showing significant decrease (*P*-value <0.05, adjusted for multiple testing with the Benjamini-Hochberg procedure) in the mutant were defined as class 1 & 2.

Total RNA extraction

Total RNA was extracted from exponentially growing cells using standard hot phenol procedure, resuspended in nuclease-free H_2O (Ambion) and quantified using a NanoDrop 2000c spectrophotometer.

Northern blot

10 µg of total RNA were loaded on denaturing 1.2% agarose gel and transferred to Hybond™-XL nylon membrane (GE Healthcare). *ctt1* mRNA and U3B were detected using AMO2063 and AMO2081 oligonucleotides, respectively (see Supplementary Table S6). ^{32}P-labelled probes were hybridized overnight at 42°C in ULTRAhyb®-Oligo hybridization buffer (Ambion). Quantitation used a Typhoon Trio PhosphorImager and the ImageQuant TL v5.2 sofware (GE Healthcare).

Strand-specific RT-qPCR

Strand-specific reverse transcription (RT) reactions were performed from at least three biological replicates (unless specified), using 1 µg of total RNA and the SuperScript®II Reverse Transcriptase kit (Invitrogen), in the presence of 6,25 µg/ml actinomycin D. For each sample, a control without RT was included. Subsequent quantitative real-time PCR were performed on technical duplicates, using a LightCycler® 480 instrument (Roche). Oligonucleotides used are listed in Supplementary Table S6.

ChIP

ChIP analysis was performed from three biological replicates of strains YAM2400 (WT) and YAM2402 (*exo2⊿*) of *S. pombe*. Exponentially growing (OD_{595} 0,5) cells were fixed for 10 minutes at room temperature using formaldehyde (1% final concentration), then glycine was added (0,4 M final concentration). Antibodies used were 8WG16 (Covance) for RNAPII, H14 (Covance) for RNAPII S5-Pho, 3E10 (Millipore) for RNAPII S2-Pho, ab1791 (Abcam) for histone H3, 05-1355 (Millipore) for acetyl-H4 (Lys5/8/12/16) and 07-353 (Millipore) for acetyl-H3 (Lys14). Quantitative real-time PCR were performed in technical duplicates on a StepOnePlus™ machine (Applied Biosystems) and a LightCycler® 480 instrument (Roche). Oligonucleotides used are listed in Supplementary Table 6.

ACCESSION NUMBERS

Raw sequences have been deposited to the NCBI Gene Expression Omnibus (accession number GEO: GSE106649).

A genome browser for visualization of NET-Seq processed data is accessible at http://vm-gb.curie.fr/mw3.

ACKNOWLEDGMENTS

We thank T. Rio Frio, S. Baulande and P. Legoix-Né (NGS platform, Institut Curie), A. Lermine (bioinformatics platform, Institut Curie). We also thank Ugo Szachnowski for assistance in bioinformatics. We are grateful to all members of our labs for discussions and critical reading of the manuscript. This work has benefited from the facilities and expertise of the NGS platform of Institut Curie, supported by the Agence Nationale de la Recherche (ANR-10-EQPX-03, ANR10-INBS-09-08) and the Canceropôle Ile-de-France. A. Morillon's lab is supported by the Agence Nationale de la Recherche (REGULncRNA, DNA-Life) and the European Research Council (EpincRNA starting grant, DARK consolidator grant).

AUTHOR CONTRIBUTIONS

MW & AM conceived and designed the study. MW, MY, DH and VM performed experiments. MW, CG, MD & AM designed NGS data analysis. CG and MD performed bioinformatics analysis. MW & AM wrote the article. AM supervised the project.

CONFLICT OF INTEREST

The authors declare that they have no competing interests.

FIGURE LEGENDS

Figure 1. Attenuation of *ctt1* induction in *exo2Δ* cells upon oxidative stress correlates with antisense *XUT0794* accumulation.

A. Loss of Exo2 confers sensitivity to hydrogen peroxide. Serial 1:10 dilutions of YAM2400 (WT) and YAM2402 (*exo2Δ*) cells were dropped on solid rich medium (YES) containing or not 1 mM or 2 mM H_2O_2. Plates were incubated at the indicated temperature for 3-4 days.

B. Northern blot analysis of *ctt1* mRNA induction in WT and *exo2Δ* cells. YAM2400 (WT) and YAM2402 (*exo2Δ*) cells were grown to mid-log phase in rich medium and collected before or after addition of 1 mM H_2O_2 for 15 min. *ctt1* mRNA and U3B snoRNA were detected from total RNA using ^{32}P-labelled oligonucleotides. Numbers represent the *ctt1* mRNA/U3B ratio (ND: not determined).

C. Snapshot of RNA-Seq signals along *ctt1* in WT and *exo2Δ*. RNA-Seq data were previously published (Wery et al, 2017). Signal for the + and - strands are visualized as heatmaps in the upper and lower panels, respectively, using VING (Descrimes et al, 2015). *ctt1* mRNA and antisense *XUT0794* are represented by blue and red arrows, respectively.

D. Strand-specific RT-qPCR analysis of *ctt1* mRNA induction in WT, *exo2Δ*, *dcr1Δ* and *exo2Δ dcr1Δ* cells. Strains YAM2400 (WT), YAM2402 (*exo2Δ*), YAM2406 (*dcr1Δ*) and YAM2404 (*exo2Δ dcr1Δ*) were grown as described above. *ctt1* mRNA level was determined by strand-specific RT-qPCR from total RNA and normalized on the level of U3B snoRNA. Data are presented as mean +/- standard deviation (SD), calculated from three biological replicates. $^{*}p < 0.05$; $^{**}p < 0.01$; $^{***}p < 0.001$ upon t-test.

E. Strand-specific RT-qPCR analysis of *ctt1* mRNA and *XUT0794* induction in WT cells upon H_2O_2 treatment. YAM2400 cells grown in rich medium to mid-log phase were collected 0, 2, 5, 10, 15, 30, 45 and 60 min after addition of H_2O_2. *ctt1* mRNA and *XUT0794* were quantified as above. Relative level of each transcript in the non-induced condition (T0) was set to 1.

Figure 2. Level of *ctt1* attenuation correlates with *XUT0794* abundance.

A. Schematic representation of hammerhead ribozyme (RZ) inserted within *XUT0794*. Self-cleaving RZ was inserted at position 254 of *XUT0794*. Position of qPCR amplicons C and D is indicated.

B. Analysis of *XUT0794* upstream from and downstream to RZ insertion site. YAM2400 (WT), YAM2402 (*exo2Δ*), YAM2565 (WT + RZ) and YAM2567 (*exo2Δ* + RZ) were grown as described in Figure 1B. Strand-specific RT on *XUT0794* was performed from total RNA using oligonucleotide AMO2069. Oligonucleotides AMO2535-6 (amplicon D) and AMO2069-70 (amplicon C) were used for qPCR detection of *XUT0794* 5' and 3' fragment, respectively. Data were normalized on U3B snoRNA. For each amplicon, the normalized level of *XUT0794* in *exo2Δ* was then set to 1. Results are presented as mean +/- SD, from four biological replicates.

C. Analysis of *ctt1* mRNA levels. Strains and cultures were as above; strand-specific RT on *ctt1* mRNA was performed using oligonucleotide AMO2535; qPCR detection was performed using AMO2535-6 (amplicon D). Data were normalized on U3B levels and are presented as mean +/- SD, from four biological replicates. $^{**}p<0.01$; $^{***}p<0.001$; ns, not significant upon t-test.

Figure 3. asXUT-mediated attenuation of *ctt1* is transcriptional.

A. Schematic map of the *ctt1* locus, with positions of the qPCR oligonucleotide pairs.

B. ChIP analysis of RNAPII occupancy along *ctt1*. Strains YAM2400 (WT) and YAM2402 (*exo2Δ*) were grown as in Figure 1B. After cross-linking, chromatin extraction and sonication, RNAPII was immunoprecipitated using antibody against the CTD of its largest subunit Rpb1. Co-precipitated DNA was purified and quantified by qPCR. Data were normalized on the *act1* signal, which is not controlled to an asXUT (see Supplementary Figure 3). The dashed line indicates the background signal observed on an intergenic region of chromosome I used as negative control. Data are presented as mean +/- SD, from three biological replicates. $^{*}p<0.05$; $^{***}p<0.001$; ns, not significant upon t-test.

C-D. ChIP analysis of Ser5-P and Ser2-P occupancy along *ctt1*. RNAPII was immunoprecipitated from the same chromatin extracts as above, using antibody against the Ser5-P (**C**) or the Ser2-P (**D**) form of

Rpb1 CTD. Data normalization was as above. For each position of *ctt1*, the ratio between Ser5-P or Ser2-P and total RNAPII is shown. Data are presented as above. $^{*}p<0.05$; $^{**}p<0.01$; $^{***}p<0.001$; ns, not significant upon t-test.

Figure 4. asXUT-mediated attenuation of *ctt1* depends on HDAC.

A-B. Strand-specific RT-qPCR analysis of asXUT-mediated attenuation of *ctt1* mRNA in the presence of HDAC inhibitor. Strains YAM2400 (WT) and YAM2402 (*exo2Δ*) were grown in rich medium to mid-log phase before addition of 40 µg/ml TSA or equivalent volume of DMSO for 2 hours. TSA-treated and control cells were then collected prior or after addition of H_2O_2 for 15 min. *ctt1* mRNA (**A**) and *XUT0794* (**B**) were quantified as described above. Data are presented as mean +/- SD, from three biological replicates.

C-D. ChIP analysis of H4K5/8/12/16 (**C**) and H3K14 (**D**) acetylation along *ctt1*. Culture, cross-linking and chromatin extraction were as described in Figure 3B. For each position, data were first normalized on *act1*, then on the level of histone H3, immunoprecipitated from the same chromatin. Probe dg is specific for the centromeric *dg* elements. Data are presented as mean +/- SD, from three biological replicates. $^{*}p<0.05$; $^{**}p<0.01$; $^{***}p<0.001$; ns, not significant upon t-test.

Figure 5. Antisense XUT stabilization induces transcriptional attenuation of a class of highly expressed genes.

A. Transcriptional attenuation in *exo2Δ* cells. NET-Seq analysis was performed in biological duplicates of WT and *exo2Δ* cells. Data for the WT strain were previously described (Wery et al, 2017). After sequencing, differential analysis discriminated genes showing significant ($P<0.05$) reduction of transcription (classes 1-2) or not (classes 3-4). Among them, classes 1 and 3 have asXUT. The number of genes for each class is indicated.

B. Box-plot of nascent transcription (NET-Seq) signal for class 1-4 genes in WT (dark grey boxes) and *exo2Δ* (Δ; light grey boxes).

C. Metagene view of NET-Seq signals along class 1 and 3 genes in WT cells. For each class, normalized coverage (tag/nt, log_2) along mRNA transcription start site (TSS) +/- 1000 nt (+ strand) and the antisense (as) strand were piled up, in a strand-specific manner. Average signal for the sense and antisense strands was plotted for class 1 (red) and class 3 (green). The shading surrounding each line denotes the 95% confidence interval.

D. Same as above in *exo2Δ* cells.

E. Density-plot showing the global NET-Seq (dashed lines) and total RNA-Seq (solid lines) signals for XUTs in the WT (black) and *exo2Δ* (pink) strains. Total RNA-Seq data were previously described (Wery et al, 2017).

F. Metagene view of nascent antisense transcription (NET-Seq) signal around the sense gene TSS of class 1 (red) and 3 (green) genes, in WT cells. The shading surrounding each line denotes the 95% confidence interval.

Figure 6. Class 1 genes show prominent promoter-proximal nucleosome depletion and histone acetylation in WT cells.

A. Metagene of H3 levels for class 1-4 genes in WT cells. The analysis was performed using previously published ChIP-Seq data (Wery et al, 2017). Metagene representation of signal for class 1 (red), class 2 (blue), class 3 (green) and class 4 (black) was performed as above, in a strand-unspecific manner. The shading surrounding each line denotes the 95% confidence interval.

B. Metagene view of H3K14 acetylation for class 1-4 genes in WT cells. ChIP-Seq libraries construction and sequencing were previously described (Wery et al, 2017). Metagene representation of signal for each class of genes was performed as above, using ratio of coverage (log_2) for H3K14ac and H3.

C. Same as above for H4K5/8/12/16ac (H4ac).

Figure 7. Regulatory threshold model.

Antisense XUT can attenuate highly transcribed genes displaying prominent promoter-proximal nucleosome depletion and high levels of histone acetylation (class 1), but not genes showing low/basal transcription, with poor nucleosome depletion and low histone acetylation (class 3). See main text for details.

SUPPLEMENTARY FIGURE LEGENDS

Supplementary Figure S1. *ctt1* mRNA induction in WT and *exo2Δ* cells does not depend on Dicer.

A. YAM2400 (WT) and YAM2402 (*exo2Δ*) cells grown in rich YES medium to mid-log phase were collected 0, 2, 5, 10, 15, 30 and 45 minutes after addition of 1 mM H_2O_2. *ctt1* mRNA was quantified from total RNA using strand-specific RT-qPCR and normalized on the level of the U3B snoRNA. Average values and standard deviations were calculated from two biological replicates.

B. T0, 2, 5 10 time points from the figure above were plotted separately and used to calculate linear trend lines. Equation and R-squared coefficient are indicated for each trend line.

C-E. WT cells with pREP-nmt1/LEU2 empty vector (pDM829, vector), and *exo2Δ* cells with pREP-nmt1/LEU2, pREPNFLAG-Dcr1 (pDM914, Dcr1) or pREPNFLAG-Dcr1-D837A,D1127A (pDM941, Dcr1*) plasmids (Yu et al, 2014) were grown to mid-log phase in EMM-Leu medium, before addition of H_2O_2 for 15 min. *ctt1* mRNA (**C**), *XUT0794* (**D**) and *dcr1* mRNA (**E**) were quantified from total RNA using strand-specific RT-qPCR and normalized on the level of the U3B snoRNA. Average values and standard deviations were calculated from two biological replicates.

Supplementary Figure S2. Effect of *XUT0794* expression in *cis* and in *trans* on *ctt1* attenuation.

A. Attenuation of *ctt1* mRNA upon overexpression of *XUT0794* in *cis*. Strains YAM2400 (WT) and YAM2474 (*P41nmt1-XUT0794*) were grown for 24 hours to mid-log phase in EMM medium +/- 15 µM thiamine, before addition of H_2O_2 for 15 min. Levels of *XUT0794* (red) and *ctt1* mRNA (blue) were quantified from total RNA using strand-specific RT-qPCR and normalized on the level of the U3B snoRNA. Data are presented as mean +/- SD from three biological replicates.

B. Induction of *ctt1* mRNA upon *XUT0794* overexpression in *trans*. YAM2475 (empty vector) and YAM2476 (pAM353; *P41nmt1-XUT0794*) cells were grown for 24 hours to mid-log phase in EMM-L medium +/- 15 µM thiamine, before addition of H_2O_2 for 15 min. Determination of *XUT0794* and *ctt1* mRNA levels and data presentation are as above.

C. Strains YAM2400 (WT), YAM2402 (*exo2Δ*) and YAM2533 (*ctt1-kan*^{R}; *kanMX6* inserted 113 bp upstream from *XUT0794*) were grown to mid-log phase in YES medium and collected prior (white bars) or after addition of 1 mM H_2O_2 for 15 min (black bars). Levels of *XUT0794* (left panel) and *ctt1* mRNA (right panel) were determined as described above. Mean values +/- SD were calculated from three biological replicates.

Supplementary Figure S3. Transcription of *act1* is not controlled by an asXUT.

Snapshot of total (input) and nascent (IP) NET-Seq signals along the *act1* gene in WT (upper panels) and *exo2Δ* (lower panels) cells. In each panel, the signal corresponding to the sense (+) and antisense (-) strand is shown in blue and pink, respectively. Blue arrows and boxes represent the mRNAs and coding sequences, respectively. NET-Seq data for the WT strain were previously described (Wery et al, 2017). The snapshot was produced using VING (Descrimes et al, 2015).

Supplementary Figure 4. Analysis of asXUT-mediated attenuation of *ctt1* in HDAC mutants.

A. Effect of Clr3 class II HDAC on XUT-mediated *ctt1* mRNA attenuation. YAM2400 (WT), YAM2402 (*exo2Δ*), YAM2407 (*clr3Δ*) and YAM2444 (*exo2Δ clr3Δ*) cells were grown in rich medium before (white) or after addition of 1 mM H_2O_2 for 15 minutes (black). *ctt1* mRNA levels were determined by strand-specific RT-qPCR from total RNA. Normalization was as above. Data are presented as mean +/- SD from three biological replicates. $^{*}p<0.05$; $^{**}p<0.01$; ns, not significant upon t-test.

B. Effect of Hos2 class I HDAC on XUT-mediated *ctt1* mRNA attenuation. Same as above using YAM2400 (WT), YAM2402 (*exo2Δ*), YAM2471 (*hos2Δ*) and YAM2472 (*exo2Δ hos2Δ*). $^{*}p<0.05$; $^{***}p<0.001$; ns, not significant upon t-test.

C. Effect of the Png2 subunit of the Clr6 HDAC complex I on XUT-mediated *ctt1* mRNA attenuation. Same as above using YAM2400 (WT), YAM2402 (*exo2Δ*), YAM2561 (*png2Δ*) and YAM2562 (*exo2Δ png2Δ*). $^{*}p<0.05$; $^{**}p<0.01$; $^{***}p<0.001$; ns, not significant upon t-test.

Supplementary Figure S5. Antisense XUT stabilization induces transcriptional attenuation of a class of highly expressed genes.

A. Global RNAPII transcription in WT and *exo2Δ* cells. Density plot of *exo2Δ*/WT NET-Seq signal ratio for mRNAs (blue), sn(o)RNAs (black) and XUTs (red).

B. Metagene view of NET-Seq signals along class 1-4 genes in WT cells. For each class, normalized signal (tag/nt, $\log_2$) along mRNA transcription start site (TSS) +/- 1000 nt (sense strand) and the antisense (as) strand were piled up, in a strand-specific manner. Average signal for each strand was plotted for class 1 (red), 2 (blue), 3 (green) and 4 (black). The shading surrounding each line denotes the 95% confidence interval.

C. Box-plot of NET-Seq signal (tag/nt, $\log_2$) for XUTs antisense to class 1 and class 3 genes in WT and *exo2Δ* (Δ) cells.

D. Metagene view of nascent antisense transcription (NET-Seq) signal around the sense gene TSS of class 1-4 genes, in WT cells. The shading surrounding each line denotes the 95% confidence interval.

References

Anders S, Huber W (2010) Differential expression analysis for sequence count data. *Genome Biol* **11**(10)**:** R106

Berretta J, Pinskaya M, Morillon A (2008) A cryptic unstable transcript mediates transcriptional trans-silencing of the Ty1 retrotransposon in S. cerevisiae. *Genes Dev* **22**(5)**:** 615-626

Bitton DA, Grallert A, Scutt PJ, Yates T, Li Y, Bradford JR, Hey Y, Pepper SD, Hagan IM, Miller CJ (2011) Programmed fluctuations in sense/antisense transcript ratios drive sexual differentiation in S. pombe. *Mol Syst Biol* **7:** 559

Calvo IA, Garcia P, Ayte J, Hidalgo E (2012) The transcription factors Pap1 and Prr1 collaborate to activate antioxidant, but not drug tolerance, genes in response to H2O2. *Nucleic Acids Res* **40**(11)**:** 4816-4824

Camblong J, Beyrouthy N, Guffanti E, Schlaepfer G, Steinmetz LM, Stutz F (2009) Trans-acting antisense RNAs mediate transcriptional gene cosuppression in S. cerevisiae. *Genes Dev* **23**(13)**:** 1534-1545

Camblong J, Iglesias N, Fickentscher C, Dieppois G, Stutz F (2007) Antisense RNA stabilization induces transcriptional gene silencing via histone deacetylation in S. cerevisiae. *Cell* **131**(4)**:** 706-717

Clark MB, Amaral PP, Schlesinger FJ, Dinger ME, Taft RJ, Rinn JL, Ponting CP, Stadler PF, Morris KV, Morillon A, Rozowsky JS, Gerstein MB, Wahlestedt C, Hayashizaki Y, Carninci P, Gingeras TR, Mattick JS (2011) The reality of pervasive transcription. *PLoS Biol* **9**(7)**:** e1000625; discussion e1001102

de Andres-Pablo A, Morillon A, Wery M (2017) LncRNAs, lost in translation or licence to regulate? *Curr Genet* **63**(1)**:** 29-33

Descrimes M, Zouari YB, Wery M, Legendre R, Gautheret D, Morillon A (2015) VING: a software for visualization of deep sequencing signals. *BMC Res Notes* **8**(1)**:** 419

Djebali S, Davis CA, Merkel A, Dobin A, Lassmann T, Mortazavi A, Tanzer A, Lagarde J, Lin W, Schlesinger F, Xue C, Marinov GK, Khatun J, Williams BA, Zaleski C, Rozowsky J, Roder M, Kokocinski F, Abdelhamid RF, Alioto T, Antoshechkin I, Baer MT, Bar NS, Batut P, Bell K, Bell I, Chakrabortty S, Chen X, Chrast J, Curado J, Derrien T, Drenkow J, Dumais E, Dumais J, Duttagupta R, Falconnet E, Fastuca M, Fejes-Toth K, Ferreira P, Foissac S, Fullwood MJ, Gao H, Gonzalez D, Gordon A, Gunawardena H, Howald C, Jha S, Johnson R, Kapranov P, King B, Kingswood C, Luo OJ, Park E, Persaud K, Preall JB, Ribeca P, Risk B, Robyr D, Sammeth M, Schaffer L, See LH, Shahab A, Skancke J, Suzuki AM, Takahashi H, Tilgner H, Trout D, Walters N, Wang H, Wrobel J, Yu Y, Ruan X, Hayashizaki Y, Harrow J, Gerstein M, Hubbard T, Reymond A, Antonarakis SE, Hannon G, Giddings MC, Ruan Y, Wold B, Carninci P, Guigo R, Gingeras TR (2012) Landscape of transcription in human cells. *Nature* **489**(7414)**:** 101-108

Drogat J, Hermand D (2012) Gene-specific requirement of RNA polymerase II CTD phosphorylation. *Mol Microbiol* **84**(6)**:** 995-1004

Giannakakis A, Zhang J, Jenjaroenpun P, Nama S, Zainolabidin N, Aau MY, Yarmishyn AA, Vaz C, Ivshina AV, Grinchuk OV, Voorhoeve M, Vardy LA, Sampath P, Kuznetsov VA, Kurochkin IV, Guccione E (2015) Contrasting expression patterns of coding and noncoding parts of the human genome upon oxidative stress. *Sci Rep* **5:** 9737

Guttman M, Amit I, Garber M, French C, Lin MF, Feldser D, Huarte M, Zuk O, Carey BW, Cassady JP, Cabili MN, Jaenisch R, Mikkelsen TS, Jacks T, Hacohen N, Bernstein BE, Kellis M, Regev A, Rinn JL, Lander ES (2009) Chromatin signature reveals over a thousand highly conserved large non-coding RNAs in mammals. *Nature* **458**(7235)**:** 223-227

Houseley J, Rubbi L, Grunstein M, Tollervey D, Vogelauer M (2008) A ncRNA modulates histone modification and mRNA induction in the yeast GAL gene cluster. *Mol Cell* **32**(5)**:** 685-695

Howe FS, Russell A, Lamstaes AR, El-Sagheer A, Nair A, Brown T, Mellor J (2017) CRISPRi is not strand-specific at all loci and redefines the transcriptional landscape. *Elife* **6**

Huber F, Bunina D, Gupta I, Khmelinskii A, Meurer M, Theer P, Steinmetz LM, Knop M (2016) Protein Abundance Control by Non-coding Antisense Transcription. *Cell Rep* **15**(12)**:** 2625-2636

Jarroux J, Morillon A, Pinskaya M (2017) History, Discovery, and Classification of lncRNAs. *Adv Exp Med Biol* **1008:** 1-46

Khalil AM, Guttman M, Huarte M, Garber M, Raj A, Rivea Morales D, Thomas K, Presser A, Bernstein BE, van Oudenaarden A, Regev A, Lander ES, Rinn JL (2009) Many human large intergenic noncoding RNAs associate with chromatin-modifying complexes and affect gene expression. *Proc Natl Acad Sci U S A* **106**(28)**:** 11667-11672

Khvorova A, Lescoute A, Westhof E, Jayasena SD (2003) Sequence elements outside the hammerhead ribozyme catalytic core enable intracellular activity. *Nat Struct Biol* **10**(9)**:** 708-712

Kief DR, Warner JR (1981) Coordinate control of syntheses of ribosomal ribonucleic acid and ribosomal proteins during nutritional shift-up in Saccharomyces cerevisiae. *Mol Cell Biol* **1**(11)**:** 1007-1015

Langmead B, Trapnell C, Pop M, Salzberg SL (2009) Ultrafast and memory-efficient alignment of short DNA sequences to the human genome. *Genome Biol* **10**(3)**:** R25

Lee JT, Lu N (1999) Targeted mutagenesis of Tsix leads to nonrandom X inactivation. *Cell* **99**(1)**:** 47-57

Lenstra TL, Coulon A, Chow CC, Larson DR (2015) Single-Molecule Imaging Reveals a Switch between Spurious and Functional ncRNA Transcription. *Mol Cell* **60**(4)**:** 597-610

Leong HS, Dawson K, Wirth C, Li Y, Connolly Y, Smith DL, Wilkinson CR, Miller CJ (2014) A global non-coding RNA system modulates fission yeast protein levels in response to stress. *Nat Commun* **5:** 3947

Libri D, Dower K, Boulay J, Thomsen R, Rosbash M, Jensen TH (2002) Interactions between mRNA export commitment, 3'-end quality control, and nuclear degradation. *Mol Cell Biol* **22**(23)**:** 8254-8266

Mercer TR, Dinger ME, Mattick JS (2009) Long non-coding RNAs: insights into functions. *Nat Rev Genet* **10**(3)**:** 155-159

Mutoh N, Nakagawa CW, Yamada K (1999) The role of catalase in hydrogen peroxide resistance in fission yeast Schizosaccharomyces pombe. *Can J Microbiol* **45**(2)**:** 125-129

Nakagawa CW, Mutoh N, Hayashi Y (1995) Transcriptional regulation of catalase gene in the fission yeast Schizosaccharomyces pombe: molecular cloning of the catalase gene and northern blot analyses of the transcript. *J Biochem* **118**(1)**:** 109-116

Nicolas E, Yamada T, Cam HP, Fitzgerald PC, Kobayashi R, Grewal SI (2007) Distinct roles of HDAC complexes in promoter silencing, antisense suppression and DNA damage protection. *Nat Struct Mol Biol* **14**(5)**:** 372-380

Pelechano V, Steinmetz LM (2013) Gene regulation by antisense transcription. *Nat Rev Genet* **14**(12)**:** 880-893

Pinskaya M, Gourvennec S, Morillon A (2009) H3 lysine 4 di- and tri-methylation deposited by cryptic transcription attenuates promoter activation. *EMBO J* **28**(12)**:** 1697-1707

Renganathan A, Felley-Bosco E (2017) Long Noncoding RNAs in Cancer and Therapeutic Potential. *Adv Exp Med Biol* **1008:** 199-222

Rinn JL, Chang HY (2012) Genome regulation by long noncoding RNAs. *Annu Rev Biochem* **81:** 145-166

Saha P, Verma S, Pathak RU, Mishra RK (2017) Long Noncoding RNAs in Mammalian Development and Diseases. *Adv Exp Med Biol* **1008:** 155-198

Schmitt AM, Chang HY (2016) Long Noncoding RNAs in Cancer Pathways. *Cancer Cell* **29**(4)**:** 452-463

Swiezewski S, Liu F, Magusin A, Dean C (2009) Cold-induced silencing by long antisense transcripts of an Arabidopsis Polycomb target. *Nature* **462**(7274)**:** 799-802

Szankasi P, Smith GR (1996) Requirement of S. pombe exonuclease II, a homologue of S. cerevisiae Sep1, for normal mitotic growth and viability. *Curr Genet* **30**(4)**:** 284-293

Uhler JP, Hertel C, Svejstrup JQ (2007) A role for noncoding transcription in activation of the yeast PHO5 gene. *Proc Natl Acad Sci U S A* **104**(19)**:** 8011-8016

Van Dijk EL, Chen CL, d'Aubenton-Carafa Y, Gourvennec S, Kwapisz M, Roche V, Bertrand C, Silvain M, Legoix-Né P, Loeillet S, Nicolas A, Thermes C, Morillon A (2011) XUTs are a class of Xrn1-sensitive antisense regulatory non coding RNA in yeast. *Nature* **475**(7354)**:** 114-117

van Werven FJ, Neuert G, Hendrick N, Lardenois A, Buratowski S, van Oudenaarden A, Primig M, Amon A (2012) Transcription of two long noncoding RNAs mediates mating-type control of gametogenesis in budding yeast. *Cell* **150**(6)**:** 1170-1181

Venkatesh S, Workman JL (2013) Set2 mediated H3 lysine 36 methylation: regulation of transcription elongation and implications in organismal development. *Wiley Interdiscip Rev Dev Biol* **2**(5)**:** 685-700

Wery M, Descrimes M, Vogt N, Dallongeville AS, Gautheret D, Morillon A (2016) Nonsense-Mediated Decay Restricts LncRNA Levels in Yeast Unless Blocked by Double-Stranded RNA Structure. *Mol Cell* **61**(3)**:** 379-392

Wery M, Gautier C, Descrimes M, Yoda M, Vennin-Rendos H, Migeot V, Gautheret D, Hermand D, Morillon A (2017) Native Elongating Transcript Sequencing reveals global anti-correlation between sense and antisense nascent transcription in fission yeast. *RNA***:** 10.1261/rna.063446.063117

Wery M, Kwapisz M, Morillon A (2011) Noncoding RNAs in gene regulation. *Wiley Interdiscip Rev Syst Biol Med* **3**(6)**:** 728-738

Xu Z, Wei W, Gagneur J, Clauder-Munster S, Smolik M, Huber W, Steinmetz LM (2011) Antisense expression increases gene expression variability and locus interdependency. *Mol Syst Biol* **7:** 468

Yap KL, Li S, Munoz-Cabello AM, Raguz S, Zeng L, Mujtaba S, Gil J, Walsh MJ, Zhou MM (2010) Molecular interplay of the noncoding RNA ANRIL and methylated histone H3 lysine 27 by polycomb CBX7 in transcriptional silencing of INK4a. *Mol Cell* **38**(5)**:** 662-674

Yu R, Jih G, Iglesias N, Moazed D (2014) Determinants of heterochromatic siRNA biogenesis and function. *Mol Cell* **53**(2)**:** 262-276

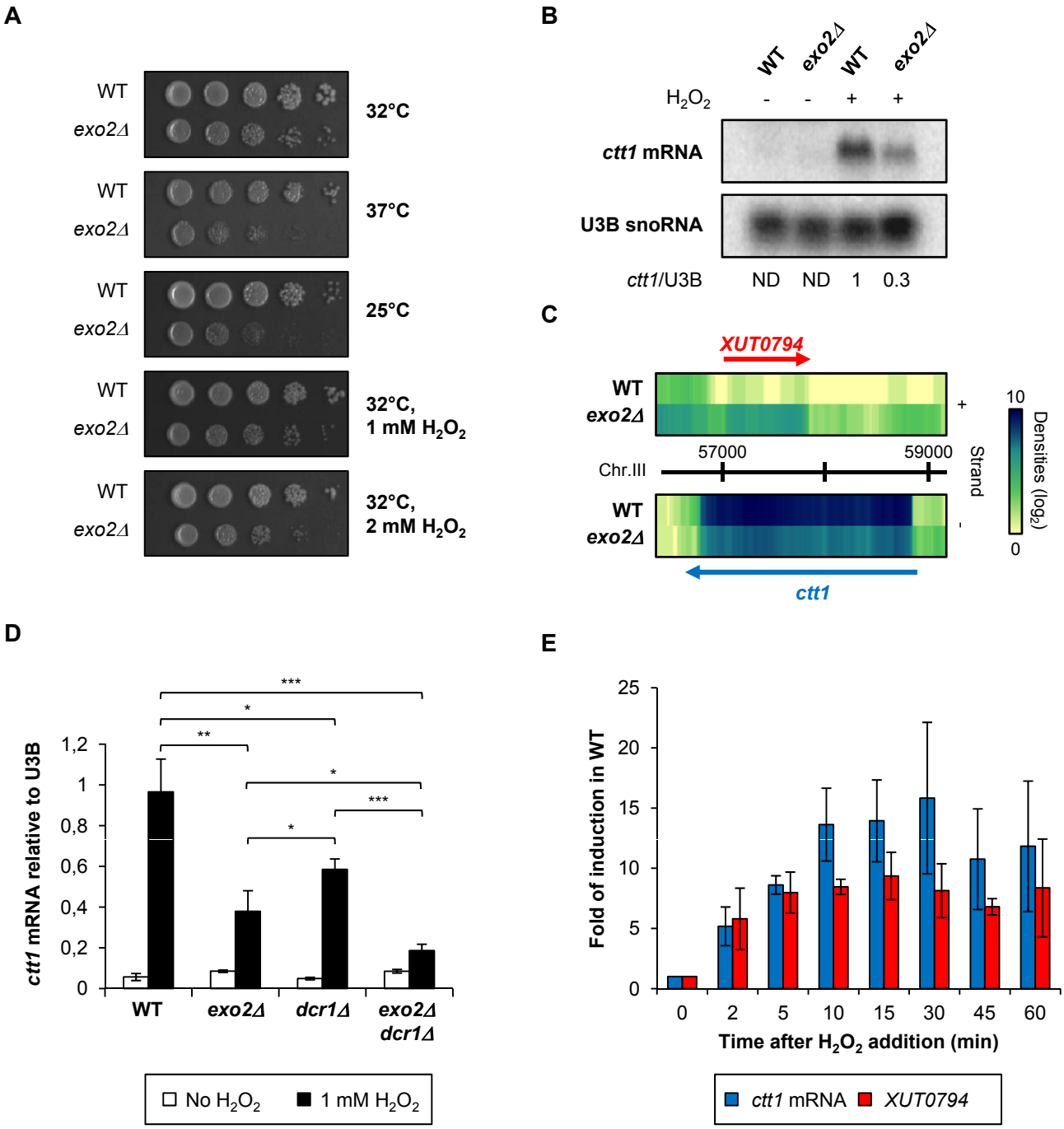

Wery_Figure 1

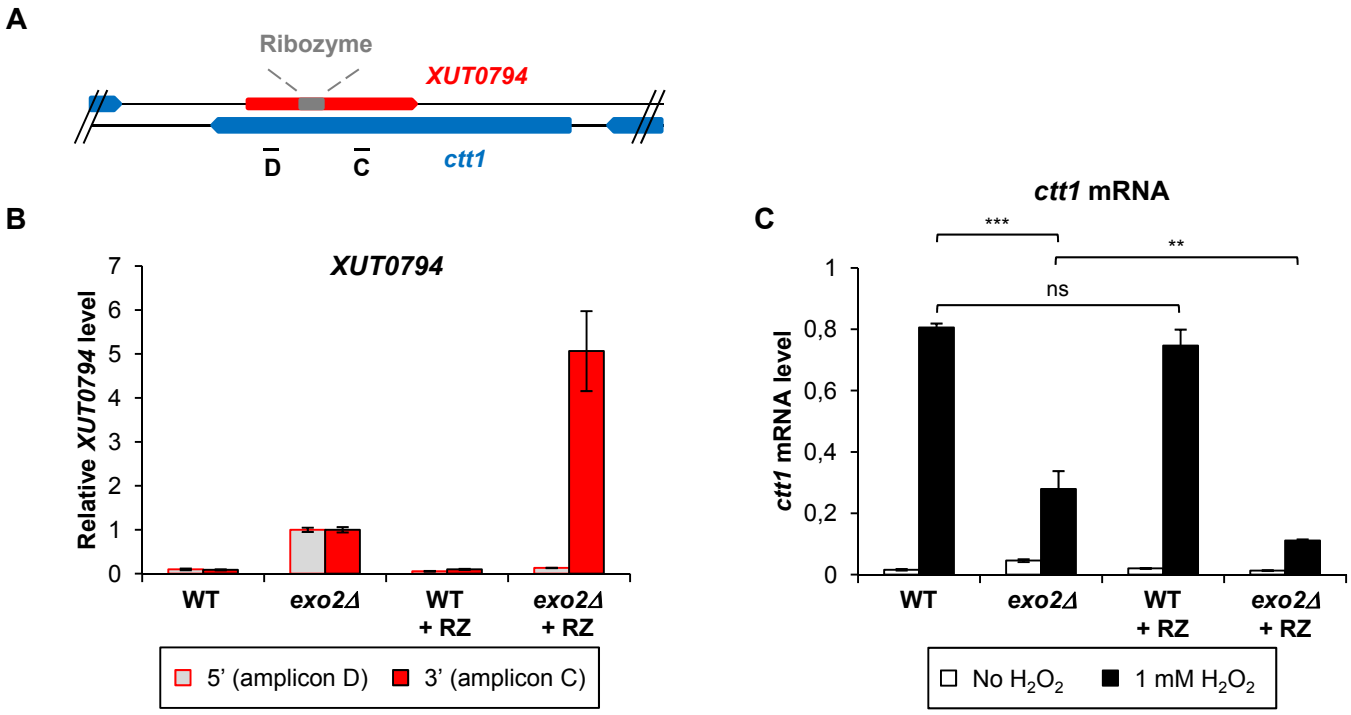

Wery_Figure 2

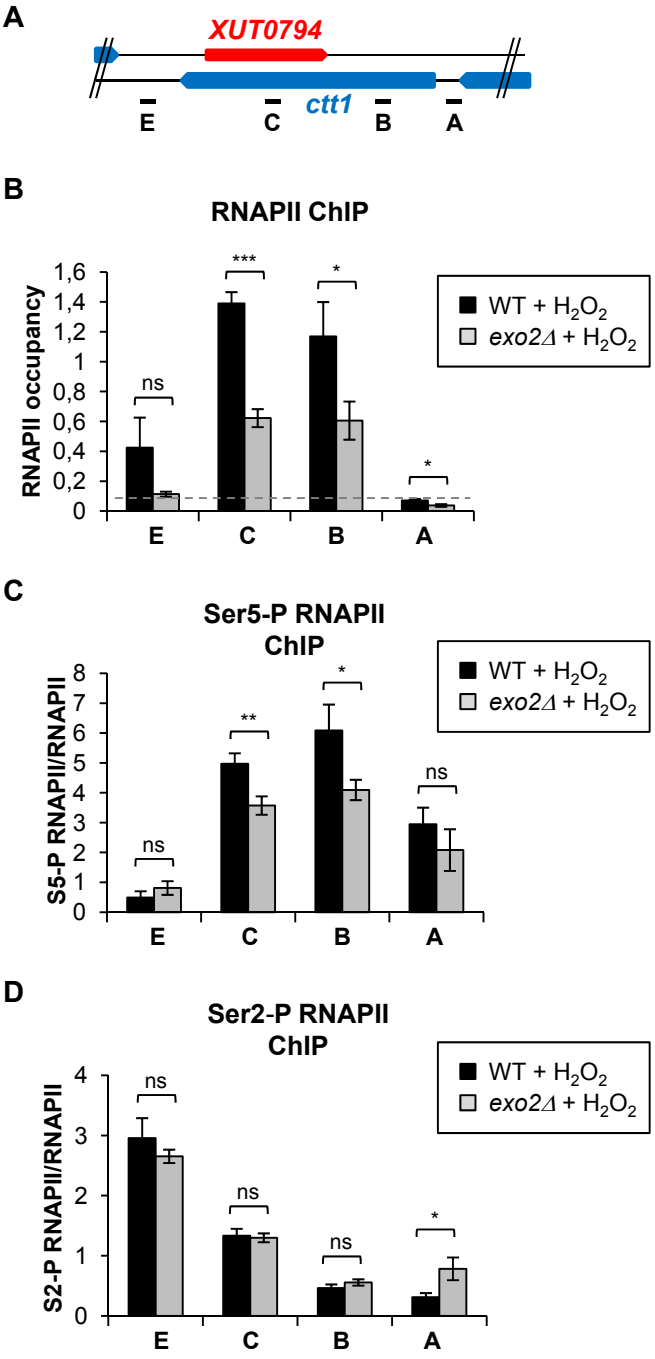

Wery_Figure 3

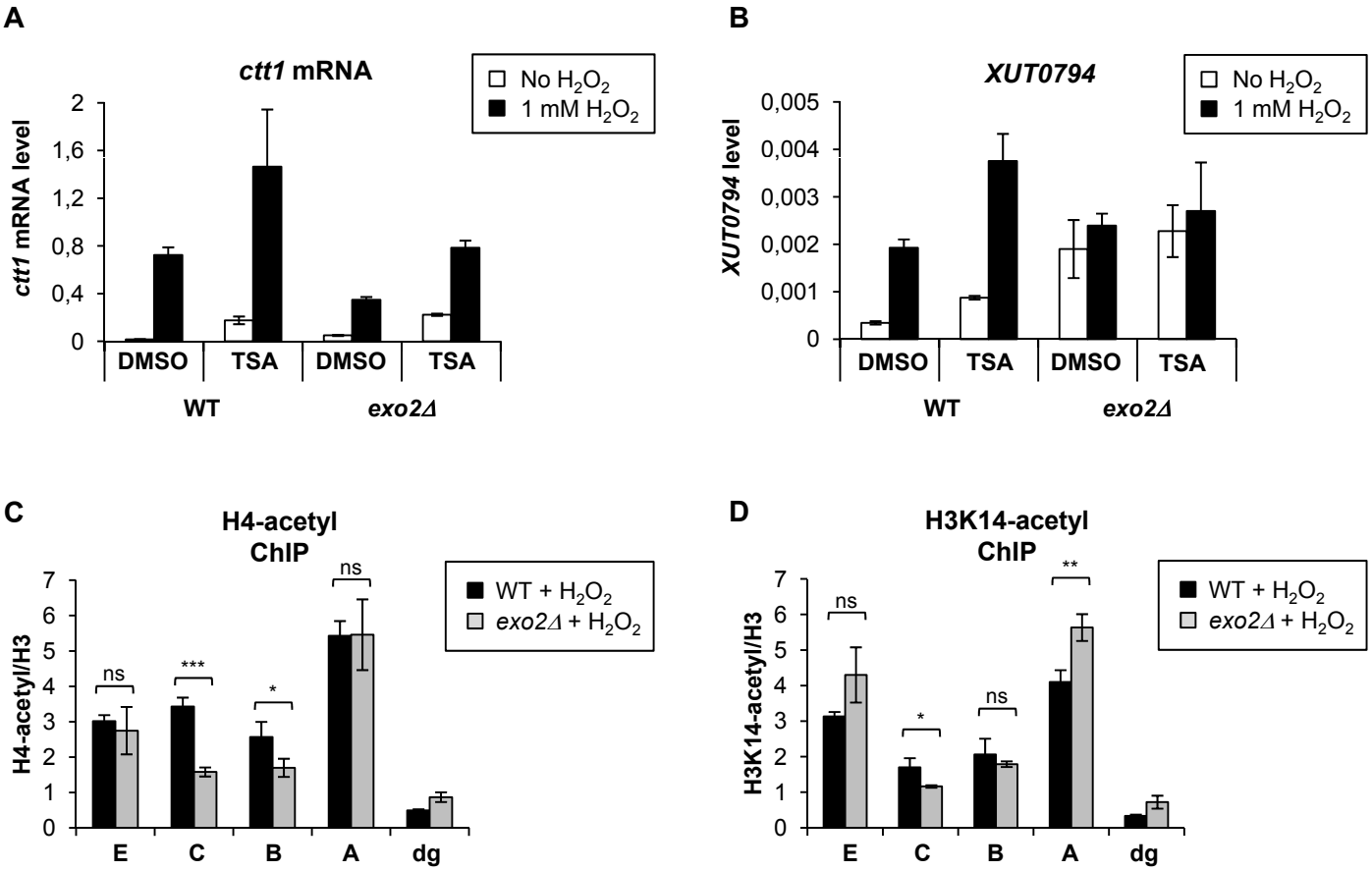

Wery_Figure 4

A

Class	asXUT	# of genes	Nascent RNA levels in *exo2Δ*
1	+	175	Down
2	-	548	Down
3	+	910	Unchanged
4	-	3495	Unchanged

B

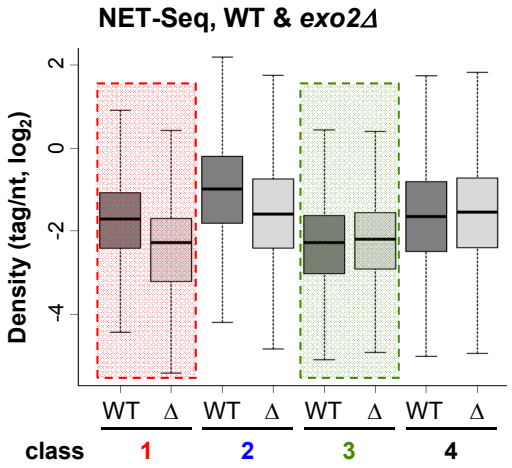

C

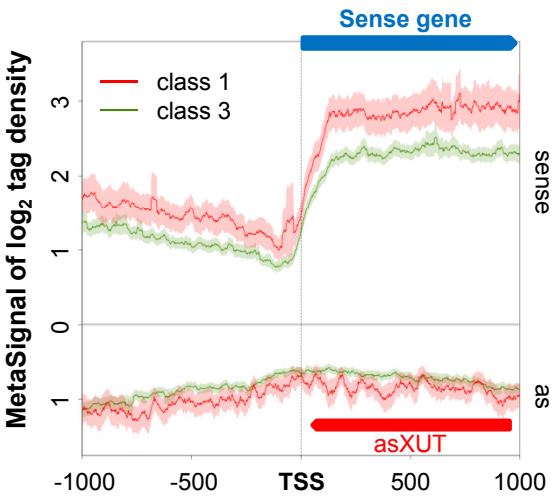

D

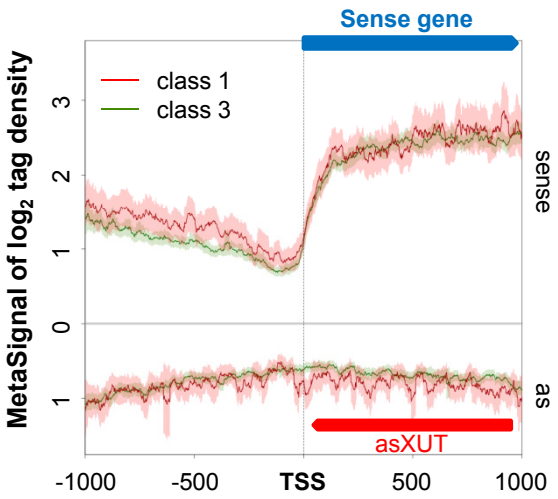

E

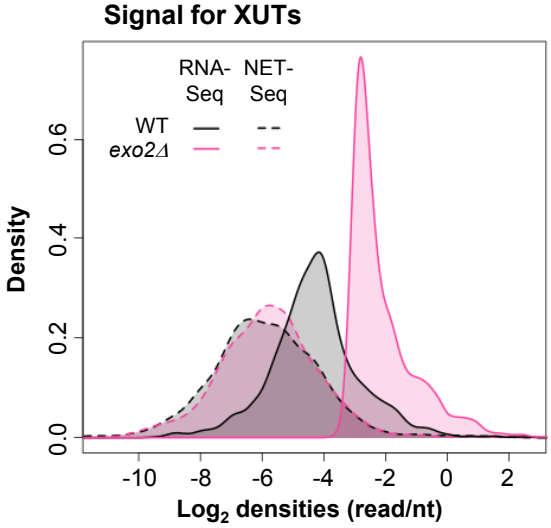

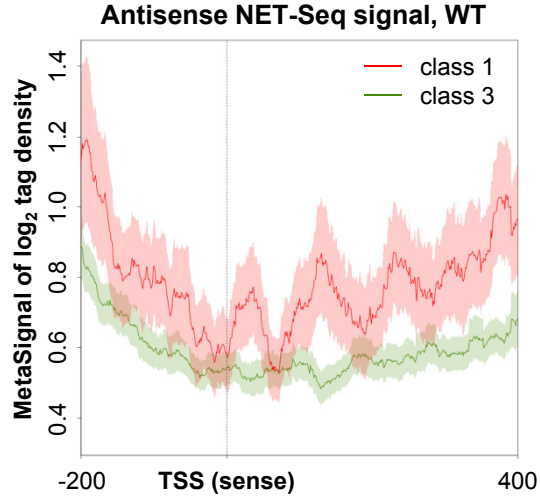

Wery_Figure 5

A

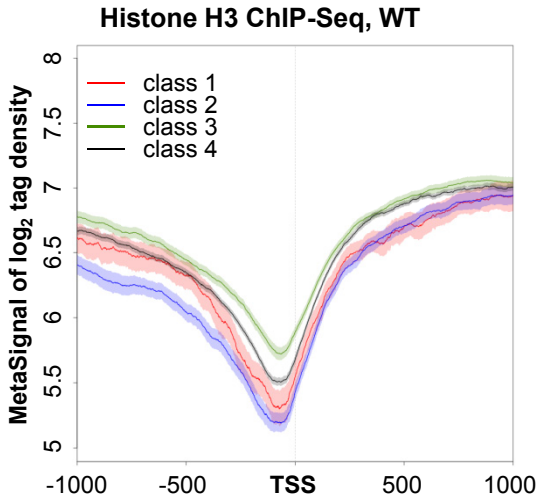

B

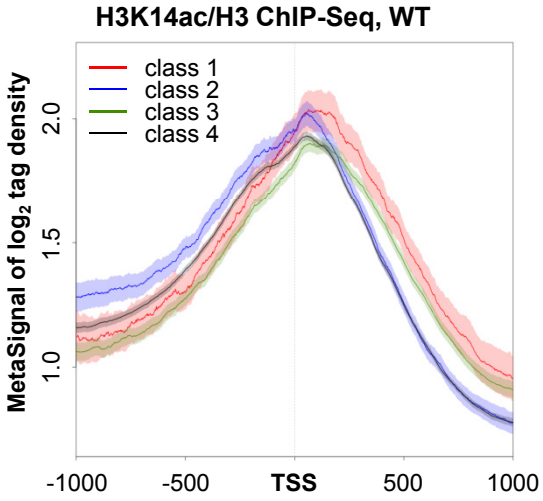

C

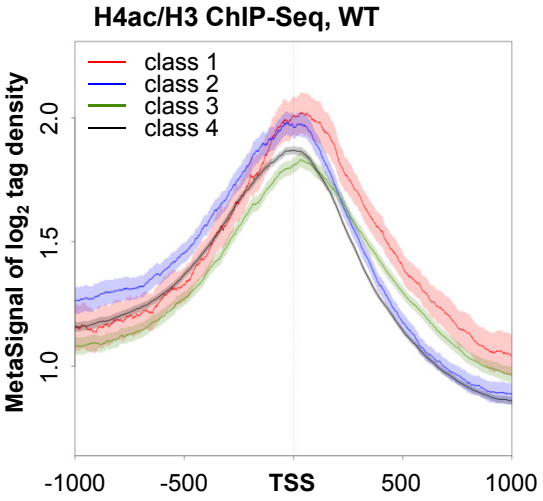

Wery_Figure 6

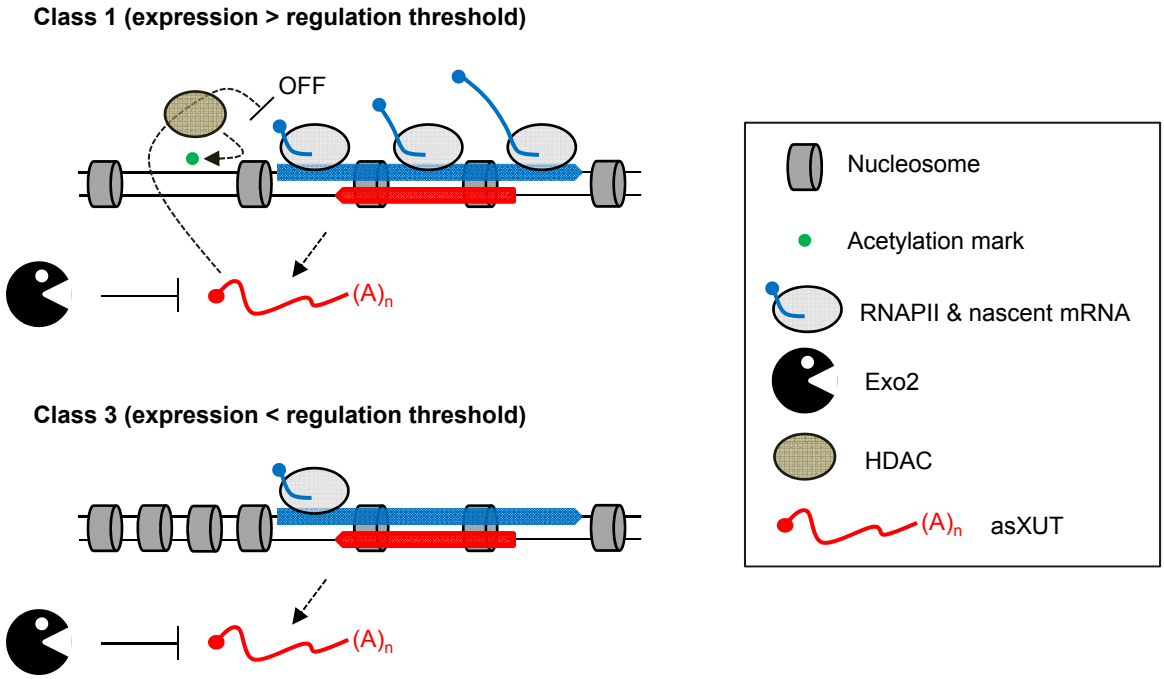

Wery_Figure 7